JOURNAL OF NEUROTRAUMA 25:1195–1205 (October 2008)

DOI: 10.1089/neu.2008.0635

Differential Hippocampal Protection when Blocking Intracellular Sodium and Calcium Entry during Traumatic Brain Injury in Rats

Xueren Zhao,[1] Fredric A. Gorin,[2] Robert F. Berman,[1] and Bruce G. Lyeth[1]

Abstract

This study investigated the contributions of the reverse mode of the sodium-calcium exchanger (NCX) and the type 1 sodium-proton antiporter (NHE-1) to acute astrocyte and neuronal pathology in the hippocampus following fluid percussion traumatic brain injury (TBI) in the rat. KB-R7943, EIPA, or amiloride, which respectively inhibit NCX, NHE-1, or NCX, NHE-1, and ASIC1a (acid-sensing ion channel type 1a), was infused intraventricularly over a 60-min period immediately prior to TBI. Astrocytes were immunostained for glial fibrillary acidic protein (GFAP), and degenerating neurons were identified by Fluoro-Jade staining at 24 h after injury. Stereological analysis of the CA2/3 sub-regions of the hippocampus demonstrated that higher doses of KB-R7943 (2 and 20 nmoles) significantly reduced astrocyte GFAP immunoreactivity compared to vehicle-treated animals. EIPA (2–200 nmoles) did not alter astrocyte GFAP immunoreactivity. Amiloride (100 nmoles) significantly attenuated the TBI-induced acute reduction in astrocyte GFAP immunoreactivity. Of the three compounds examined, only amiloride (100 nmoles) reduced hippocampal neuronal degeneration assessed with Fluoro-Jade. The results provide additional evidence of acute astrocyte pathology in the hippocampus following TBI, while suggesting that activation of NHE-1 and the reverse mode of NCX contribute to both astrocyte and neuronal pathology following experimental TBI.

Key words: astrocyte; glia; hippocampus; ion exchangers; lateral fluid percussion injury; neuronal degeneration; sodium; traumatic brain injury.

Introduction

Research on traumatic brain injury (TBI) and ischemia has typically focused on injury to neurons, although astrocyte damage has been documented to occur as a consequence of central nervous system (CNS) injury and is likely to contribute importantly to the pathophysiology of brain injury (Floyd and Lyeth, 2007). Previous experimental studies have shown disruption of key markers of astrocyte structure (e.g., glial fibrillary acidic protein [GFAP]) and function (e.g., glutamine synthetase) in selectively vulnerable brain regions within 24 h after lateral fluid percussion TBI in rats (Zhao et al., 2003). The reduction in GFAP immunoreactivity within hours after fluid percussion TBI is also associated with reduction in immunoreactivity for glutamine synthetase, another astrocyte-specific enzyme which catalyzes the formation of glutamine from glutamate. These immunocytochemical alterations are associated with morphological reduction in fine vellate process complexity with fewer processes and reduced astrocyte branching (Zhao et al., 2003). These observations are consistent with other *in vivo* studies indicating that astrocytes are vulnerable to both TBI and ischemia (Liu et al., 1999; Ouyang et al., 2007; Zhao et al., 2003). Exposing cultured astrocytes to an excitotoxic glutamate (1 mM) condition also produces acute alterations characterized by fewer processes and reduced, diffuse GFAP immunostaining (Noble et al., 1992). Those results are consistent with similar findings in transient forebrain ischemia in which immunoreactivity for GFAP was transiently reduced in the absence of astrocyte death (Ouyang et al., 2007). More severe insults such as permanent middle cerebral artery occlusion in rats produces early astrocyte cell loss that precedes neuronal cell death (Liu et al., 1999).

Astrocytes play many important roles in normal brain function including termination of excitatory signaling by transport of glutamate away from the synapse. The importance of astrocyte function following TBI has been clearly

Departments of [1]Neurological Surgery and [2]Neurology, University of California at Davis, Davis, California.

shown in a study of proliferating, reactive astrocytes which typically occurs days after injury. Targeted ablation of dividing reactive astrocytes increased neuronal degeneration and inflammation following controlled cortical impact in mice (Myer et al., 2006). The major glutamate transport mechanisms are the astrocyte-specific sodium-dependent glutamate transporters, GLT-1 and GLAST (Danbolt, 1994, 2001; Takahashi et al., 1997). Numerous studies have demonstrated a many-fold increase in extracellular glutamate immediately following TBI (Faden et al., 1989; Globus et al., 1995; Katayama et al., 1990; Zhong et al., 2006). Astrocytes protect neurons by reuptake of glutamate using electrogenic, sodium-dependent glutamate transporters and thus, experience increased intracellular sodium ($[Na^+]_i$) following TBI. Excessive elevation of $[Na^+]_i$ leads to cell swelling (Kimelberg, 1992; Kimelberg et al., 1992) and intracellular acidosis (Kempski et al., 1990). Also, magnetic resonance spectroscopy studies demonstrate a decrease in brain intracellular pH immediately after moderate fluid percussion TBI in rats that lasts for up to ninety minutes (McIntosh et al., 1987; Vink et al., 1987). Intracellular acidosis in astrocytes activates the type 1 sodium-hydrogen antiporter (NHE-1) (Grinstein and Rothstein, 1986) leading to further accumulation of $[Na^+]_i$. Thus, sodium-dependent glutamate transport and NHE-1 activation respond immediately following TBI to dually elevate $[Na^+]_i$. Excessive elevation of $[Na^+]_i$ can initiate reversal of the forward mode of the sodium-calcium exchanger (NCX) in astrocytes to import potentially cytotoxic levels of intracellular calcium (Bondarenko and Chesler, 2001; Floyd et al., 2005). Following TBI excessive glutamate transport, activation of NHE-1, and reversal of the NCX could all contribute towards disrupting normal astrocyte function and contribute towards additional neuronal excitotoxicity through compromise of normal astrocytic functions (e.g., glutamate transport). Previously, we have demonstrated that mechanically damaged primary astrocytes accumulate $[Na^+]_i$ and that subsequent damage could be prevented by blocking either glutamate transport or the reverse mode of NCX (Floyd et al., 2005).

The present study examines issues related to ion transport/exchange and acute cellular pathology using an *in vivo* TBI model. Experiments examine the effects of pharmacological inhibition of NCX and NHE-1 on acute astrocyte pathology and acute neuronal degeneration following fluid percussion TBI in rats. Results indicate amiloride, a compound that inhibits NHE-1, NCX, and ASIC1a (acid-sensing ion channel type 1a) is more effective in reducing cellular pathology than compounds selectively targeting a single antiporter.

Methods

Subjects

A total of 84 male Sprague-Dawley rats (Harlan, Indianapolis, IN) weighing 340 ± 15 g were used. Animals were housed in individual cages in a temperature (22°C) and humidity-controlled (50% relative) animal facility with a 12-h light/dark cycle (light cycle 0600/1800 h). Water was continually available. All animal procedures were approved by the University of California, Davis, Institutional Animal Care and Use Committee.

Surgical procedure

Rats were anesthetized with 4% isoflurane in a 2:1 nitrous oxide/oxygen mixture, intubated, and mechanically normoventilated with a rodent volume ventilator (model 683; Harvard Apparatus, Holliston, MA) with isoflurane reduced to 2%. Rats were mounted in a stereotaxic frame, a scalp incision made along the midline, and a 4.8-mm-diameter craniectomy was performed with a trephine on the right parietal bone (centered at −4.5 mm Bregma and right lateral 3.0 mm). A rigid plastic injury tube (modified Luer-loc needle hub, 2.6 mm inside diameter) was secured over the exposed, intact dura with cyanoacrylate adhesive. The assembly was secured to the skull with cranioplastic cement (Plastics One, Roanoke, VA) and two skull screws (2.1 mm diameter, 6.0 mm length) at 1 mm rostral to Bregma and 1 mm caudal to Lambda. Rectal temperature and temporalis muscle temperature were continuously monitored and maintained within normal ranges during surgical preparation by a feedback temperature controller pad (CMA model 150; CMA/Microdialysis AB, Solna, Sweden).

Drug administration

All drugs were dissolved in DMSO, diluted 1:9 v/v in artificial cerebrospinal fluid (7.2 pH) and stored at −20°C in aliquots for individual use. KB-R7943 (2-[2-[4-(4-nitrobenzyoxyl)phenyl]]isothiourea mesylate; Tocris Bioscience no. 1244) was used to inhibit NCX; EIPA (5-(N-Ethyl-N-isopropyl) amiloride; A-3805, Sigma-Aldrich) was used to inhibit NHE-1; amiloride hydrochloride (A-7410, Sigma-Aldrich) was used to inhibit NHE-1, NCX, and ASIC1a. Separate groups of rats were injected intracerebroventricularly (ICV) with either 0.2, 2.0, or 20 nmoles of KB-R7943; or 2.0, 20, or 200 nmoles of EIPA; or 100 nmoles of amiloride. These drug dosages were based on preliminary experiments to determine maximum tolerable dosages. All drugs and drug-vehicles were injected ICV in a total volume of 20 μL infused over a 60-min period immediately prior to TBI using a 100-μL glass microsyringe (model 81001; Hamilton Co., Reno, NV) and microinfusion pump (model 100; KD Scientific, Holliston, MA). Injections were made stereotaxically (-1.0 mm posterior from Bregma, 1.6 mm lateral from midline, and 3.6 mm below the superior skull surface) into the left lateral ventricle through a 2.0-mm-diameter craniotomy in the left parietal bone, contralateral to the fluid percussion craniectomy. The drug infusion craniectomy was filled with bone wax (item W31G; Ethicon, Somerville, NJ) and covered with cranioplastic cement prior to delivery of the lateral fluid percussion injury pulse.

Traumatic brain injury

Experimental TBI was produced using a fluid percussion device (VCU Biomedical Engineering, Richmond, VA) (Dixon et al., 1987) using the lateral orientation (Mcintosh et al., 1989). The device consists of a Plexiglas cylindrical reservoir filled with isotonic saline. One end of the reservoir has a Plexiglas piston mounted on O-rings, and the opposite end has a transducer housing with a 2.6-mm-inside-diameter male Luer-loc opening. Injury was induced by the descent of a pendulum striking the piston, which injects a small volume of saline epidurally into the closed cranial cavity. This

results in a brief displacement and deformation of neural tissue. The pressure pulse was measured in atmospheres (ATM) by an extracranial transducer (model EPN-0300A*-100A; Entran Devices, Inc., Fairfield, NJ) and recorded on a digital storage oscilloscope (model TDS 1002; Tektronix Inc., Beaverton, OR).

The rats were disconnected from the ventilator, the injury tube connected to the fluid percussion cylinder, and a moderate fluid percussion pulse (defined as 2.25 atmospheres) was delivered within 10 sec. Immediately after TBI, rats were again ventilated with a 2:1 nitrous oxide/oxygen mixture without isoflurane. The plastic injury tube and skull screws were removed, and the scalp incision was closed with 4.0 braided silk sutures. As soon as spontaneous breathing was observed, the animal was extubated and returned to its cage for post-injury observation.

One group of rats ($n = 4$) designated as "sham" underwent all surgical and anesthesia procedures described above, except that no fluid pulse was delivered to the brain. These animals served as an uninjured control group in the GFAP analysis in Experiment 1.

Tissue collection and sectioning

Rats were euthanized at 24 h after TBI by deep sodium pentobarbital anesthesia (100 mg/kg intraperitoneal) followed by transcardial perfusion with 100 mL of 0.1 M sodium phosphate buffer (PB; pH = 7.4), followed by 350 mL of 4% paraformaldehyde (pH 7.4). Brains were removed and stored overnight in 4% paraformaldehyde at 4°C. Coronal sections were cut at 50 μm thickness with a vibratome (Pelco Vibratome 1000; Ted Pella Inc., Redding, CA). Every serial section starting at –2.12 mm Bregma and ending at –4.80 mm Bregma was saved in 24-well cell culture plates for later staining. Systematic random sampling techniques were used for selecting tissue sections for staining and stereological analysis. Every fifth section was sampled starting at a section randomly determined from the first through fifth rostral-most sections. A total sample of 10 sections was selected for GFAP immunostaining. An additional set of 10 adjacent sections were used for Fluoro-Jade histofluorescent staining.

Immunohistochemistry

GFAP immunolocalization was carried out by immunohistochemistry. Free-floating tissue sections (50 μm) were washed three times (3 min each) in 0.1 M PB with agitation. Sections were incubated in 1.5% horse serum containing 0.3% Triton X-100 in 0.1 M PB for 1 h at 37°C. The sections were then transferred without washing and incubated with anti-GFAP antibody (monoclonal, mouse, 1:2000; ICN Biomed. Inc., Aurora, OH) in PB for 1 h at room temperature on a shaker followed by 24-h incubation at 37°C. After three washes (10 min each) in PB, the sections were then incubated in secondary antibody (horse anti-mouse IgG; Vector Laboratories, Burlingame, CA) for 10 min on a shaker at room temperature followed by 1 h at 37°C. Sections were then washed three times in PB (3 min each) and incubated with avidin-biotin-peroxidase complex (Vectastain Elite ABC kit PK6102; Vector Laboratories) for 2 h at room temperature. Following three washes in PB (3 min each), the sections were visualized in Vector SG substrate kit for peroxidase (SK-4700; Vector Laboratories). The reaction was stopped by transferring the sections into PB, following by two 5-min washes in PB with agitation. Finally, the sections were mounted on gelatin-chrome alum-coated glass slides and allowed to dry in air, and then dehydrated serially in alcohol and cover-slipped with DePeX mounting medium (Electron Microscopy Sciences, Fort Washington, PA). The immunolabeled products were visible as blue/gray stained cells under a light microscope with distinct astrocyte cell morphology. Control immunostaining experiments included identical immunohistochemistry procedures but without the primary antibody and another without the secondary antibody.

Fluoro-Jade histofluorescence

Tissue sections were mounted onto gelatin-chrome alum-coated slides in distilled water and air-dried overnight. The slide-mounted tissue sections were immersed subsequently in 100% alcohol (3 min), 70% alcohol (1 min), dH_2O (1 min), and 0.006% potassium permanganate (15 min). Sections were rinsed in dH_2O (1 min), incubated in the dark in 0.001% Fluoro-Jade B (Histo-Chem Inc., Pine Bluff, AK) staining solution in 0.1% acetic acid for 30 min, rinsed again for 3 min in dH_2O, and air-dried. Finally, the sections were immersed in xylene and cover-slipped with DePeX mounting medium. Sections stained with Fluoro-Jade were examined under ultraviolet (UV) light with a FITC fluorescence filter cube (Nikon B-2A, Tokyo, Japan). Stained with Fluoro-Jade, neurons undergoing degeneration brightly fluoresced in comparison to the background (Schmued et al., 1997; Schmued and Hopkins, 2000).

Anatomical regions of interest examined for histopathology

The dorsal CA2/3 regions of the hippocampus were selected as the anatomical region of interest because of this region's importance in learning and short-term memory, which are impaired following TBI. The CA2/3 regions demonstrate reliable and consistent patterns of altered astrocyte immunoreactivity (Zhao et al., 2003) and neuronal degeneration following lateral fluid percussion TBI (Hallam et al., 2004). In contrast, the CA1 and dentate gyrus show variable degrees of neuronal degeneration, while reduction of GFAP immunoreactivity is minimal (Hallam et al., 2004; Zhao et al., 2003). Similarly, neuronal degeneration in the lateral cerebral cortex is comparatively more variable than in the CA2/3 and is often characterized by frank tissue destruction (infarction), preventing accurate stereological counting of individual GFAP-positive astrocytes and degenerating neurons (Hallam et al., 2004).

Stereological counts of astrocytes were made in the dorsal hippocampus from coronal sections between Bregma –2.12 mm through –4.80 mm in the hemisphere ipsilateral to the craniectomy on the right parietal bone (injury side) and in the contralateral hemisphere. To optimize stereological quantification, astrocytes were counted in brain regions bounded by the alveus surrounding the CA2 and CA3, and a line tangent to the lateral tips of the granule cell layer of the superior and inferior blades of the dentate gyrus as described previously (Zhao et al., 2003). In the rostral-most sections (e.g., Bregma −2.12 mm through 2.20 mm), the region of interest was the CA3 bounded by the alveus and the granule cell layer of the superior blade of the dentate gyrus. These

procedures for defining regions of interest resulted in the majority of sections caudal to Bregma –2.20 also including a small segment of the lateral CA1. Criterion for counting astrocytes included morphologically distinct cell bodies and clearly identifiable astrocyte foot projections.

Stereological counts of degenerating neurons were made in the same general regions of interest as astrocytes but were further restricted to the neuron-rich stratum pyramidale in the hemisphere ipsilateral to the craniectomy. Degenerating neurons were identified as Fluoro-Jade-positive green fluorescing, morphologically distinct neuronal cell bodies with at least one clearly identifiable dendrite.

Stereological cell counts

A single investigator (X.Z.) collected all stereological data for the study without knowledge of the treatment group identity of each rat. The total number of astrocytes and degenerating neurons within the region of interest was assessed using the optical fractionator technique (West et al., 1991) with the computer-based Stereologer™ system (version 1.3; Systems Planning & Analysis, Inc., Alexandria, VA). The equipment consisted of a microscope (E600; Nikon, Tokyo, Japan) with a motorized stage (MS-2000; Applied Scientific Instruments, Eugene, OR) and color CCD camera (LE-470; Optronics, Goleta, CA). The camera's digital output was processed by a high-resolution video card (Bandit; Coreco Inc., St. Laurent, Quebec) and displayed on a computer monitor (PF 775; Viewsonic, Walnut, CA). The Stereologer™ software controlled operation of the system. The optical fractionator technique combines the optical dissector method described by Sterio (1984) and the fractionator method described by Gundersen (1986), and permits unbiased estimates of numbers of objects in a three-dimensional space. The optical dissector method counts objects within three-dimensional probes (dissectors) placed uniformly and isotopically through the entire reference space. The fractionator method calculates the total number of objects in the entire reference space by summing the objects sampled in the individual dissectors and multiplying by the reciprocals of the sampling fractions for section (SSF), area (ASF), and thickness (TSF) of the reference space. This procedure insured that each astrocyte or degenerating neuron within the reference space had an equal probability of being sampled and that each cell could be sampled only once.

The sampling parameters used for estimate of cell number in each animal were as follows: SSF = 0.20 (10 sample sections out of 50 total sections), the height of each dissector was 5.0 μm, the guard height was 0.2 μm, the TSF averaged 0.70 (dissector height/tissue section thickness), the dissector frame area was set at 50% (screen height)^2 yielding a counting frame area of 0.0068 mm^3, and the ASF was 0.076 (dissector frame area/square of the distance between dissectors). Dissectors spaced 300 μm apart were randomly generated by the Stereologer™ program. A 2× objective (Plan Apo, NA 0.10, Nikon; on-screen magnification = 161×) was used to outline the region of interest. Cell identification and counting were performed with a 40× objective (Plan Apo, NA 0.95, Nikon; on-screen magnification = 3138×). Astrocyte cell counts (GFAP) were made in both the ipsilateral and contralateral hippocampus. Degenerating neurons (Fluoro-Jade) were counted in the ipsilateral hemisphere since the numbers of Fluoro-Jade-positive degenerating neurons were negligible in the contralateral hippocampus at 24 h after TBI (Zhou et al., 2003).

Statistical analysis

Cell count data in the text and graphs are expressed as mean ± standard error of the mean (SEM). Data in Table 1 are expressed as mean ± standard deviation (SD). Data analysis was performed using SPSS software, which adheres to a general linear model. Alpha level for Type I error was set at 0.05 for rejecting the null hypotheses. Temperature and ATM measurements were analyzed using separate one-way analysis of variances (ANOVAs) between treatment groups.

In each of the cell counting experiments, the numbers of GFAP-immunostained astrocytes in the CA2/3 of the contralateral hippocampus of the vehicle- and drug-treated groups were analyzed using one-way ANOVA. Results in-

Table 1. Group Size, Injury Magnitude, and Temperatures

			Temperature (°C)			
			Pre-TBI		*Post-TBI*	
Treatment group	*Group size (n)*	*ATM*	*Rectal*	*Temporalis*	*Rectal*	*Temporalis*
Experiment 1						
Vehicle	10	2.25 ± 0.03	36.8 ± 0.2	36.3 ± 0.2	36.9 ± 0.3	36.3 ± 0.3
KB-R7943 0.2 nmoles	10	2.24 ± 0.02	37.2 ± 0.4	36.4 ± 0.4	37.1 ± 0.4	36.4 ± 0.4
KB-R7943 2.0 nmoles	10	2.23 ± 0.03	37.2 ± 0.4	36.4 ± 0.3	36.9 ± 0.5	36.5 ± 0.3
KB-R7943 20. nmoles	10	2.24 ± 0.03	37.0 ± 0.3	36.4 ± 0.3	36.8 ± 0.3	36.3 ± 0.4
Experiment 2						
Vehicle	7	2.26 ± 0.02	37.4 ± 0.2	36.3 ± 0.2	37.1 ± 0.5	36.2 ± 0.2
EIPA 2.0 nmoles	5	2.25 ± 0.02	37.5 ± 0.2	36.4 ± 0.1	37.4 ± 0.2	36.5 ± 0.3
EIPA 20. nmoles	6	2.27 ± 0.03	37.5 ± 0.1	36.4 ± 0.2	37.2 ± 0.3	36.3 ± 0.1
EIPA 200. nmoles	6	2.29 ± 0.02	37.3 ± 0.4	36.5 ± 0.4	37.4 ± 0.2	36.3 ± 0.2
Experiment 3						
Vehicle	8	2.25 ± 0.02	37.4 ± 0.2	36.3 ± 0.3	37.3 ± 0.5	36.2 ± 0.3
Amiloride 100 nmoles	8	2.23 ± 0.03	37.3 ± 0.1	36.1 ± 0.2	37.2 ± 0.4	36.2 ± 0.2

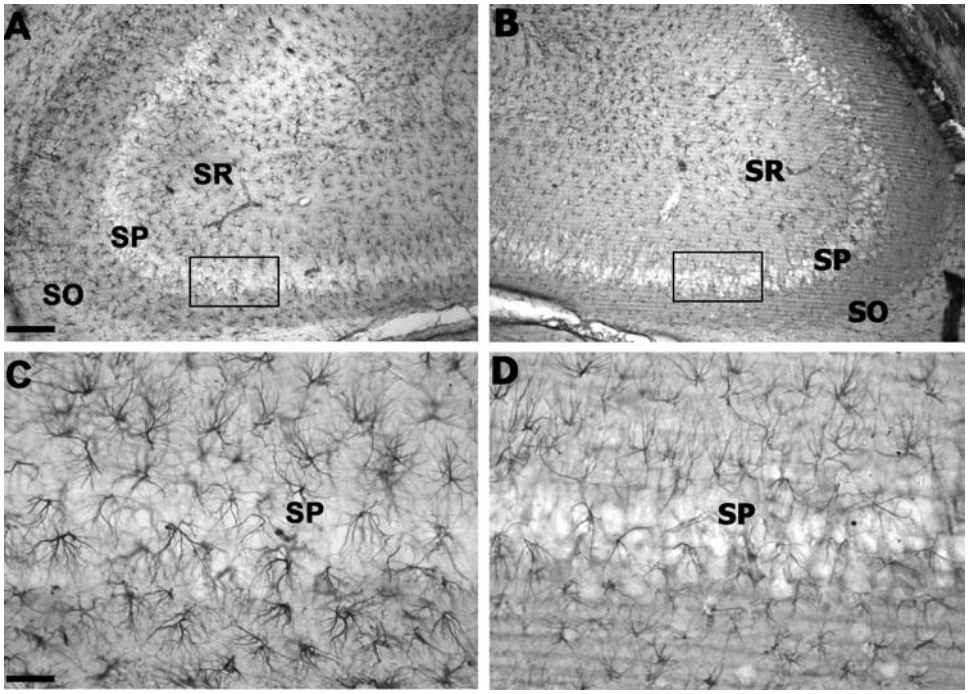

FIG. 1. GFAP immunoreactivity in hippocampus at 24 h after TBI. (**A**) Representative section from the contralateral hemisphere (Bregma −3.30 mm). (**B**) Section from the ipsilateral hemisphere of the same rat showing reduced intensity of GFAP immunostaining. (**C**) Higher magnification from the boxed area in panel A showing the morphology of astrocytes. (**D**) Higher magnification of the boxed area in B showing the reduced immunostaining and reduced numbers of intact stained astrocytes. SO, stratum oriens; SP, stratum pyramidale; SR, stratum radiatum. Scale bar = 100 μm (A,B); 10 μm (C,D).

dicated no significant differences in mean counts in the vehicle- and drug-treated groups in contralateral hemisphere of each experiment. Subsequently, in the statistical analysis of the ipsilateral hemisphere data, the contralateral vehicle-treated group from each experiment was used as the control group. Thus, in each experiment, an ANOVA was performed on the following groups: contralateral vehicle-treated (control), ipsilateral vehicle-treated, and ipsilateral drug-treated. Bonferroni corrected post-hoc comparisons were performed to determine significant differences between individual groups while holding experiment-wise error rate to 0.05.

Statistical comparisons of the numbers of Fluoro-Jade-positive ipsilateral cell counts in drug treatments groups and control (ipsilateral vehicle) were also analyzed using one-way ANOVA. In the Fluoro-Jade analysis, the ipsilateral vehicle was used as control, as Fluoro-Jade-positive cells were only rarely observed in the contralateral hippocampus. Bonferroni corrected post-hoc comparisons were performed to determine significant differences between individual groups while holding experiment-wise error rate to 0.05.

Coefficient of error (CE), defined as the SEM divided by the mean, was calculated by Stereologer^{TM} software and used as an index of the precision of cell number estimates. Pilot studies determined appropriate dissector dimensions and sampling frequency to maintain a CE level below 0.10 (i.e., 10% method error). CE values are expressed as mean ± SD.

Results

There were no significant differences between groups in injury magnitude, temporalis muscle temperature, or rectal temperature values (Table 1). Astrocyte morphology, identified by GFAP immunoreactivity, in the contralateral CA2/3 hippocampus region of interest was characterized by distinct cell somas and clearly identifiable processes (Fig. 1A,C) and was indistinguishable from shams (data not shown). In contrast, the ipsilateral injured CA2/3 contained clearly visible changes in GFAP immunoreactivity at 24 h after TBI (Fig. 1B,D). This included a loss of GFAP staining intensity with an apparent reduction in astrocyte density and fewer processes with reduced branching in the CA2/3 hippocampus region of interest compared to the contralateral region. Within the hippocampus, the reduction in GFAP immunostaining was confined generally to CA2/3 sectors. In cortex, there appeared to be reduced GFAP immunostaining coincident with areas of Fluor-Jade staining of degenerating neurons (data not shown). Quantification of GFAP-labeled astrocytes was restricted to the CA 2/3 regions of the hippocampus, while the high degree of mechanical damage within the lateral cortex made quantification of brain cell types impractical.

KB-R7943 treatment: Astrocytes

As shown in Figure 2, stereological quantification of GFAP-labeled astrocytes revealed significant differences

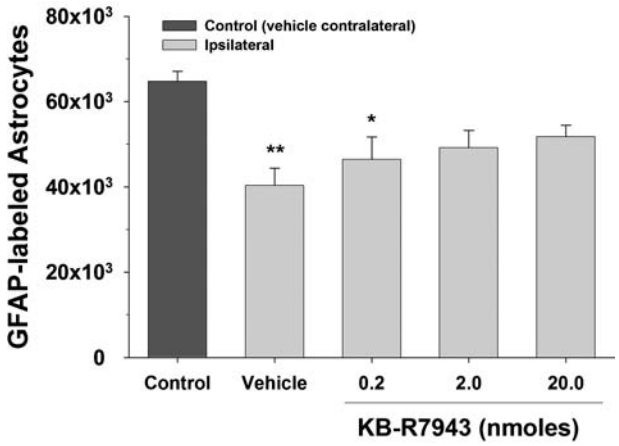

FIG. 2. Stereological quantification of GFAP-labeled astrocytes at 24 h after TBI in hippocampal CA2/3 after KB-R7943 treatment. Vehicle-treated rats and the 0.2 nmole dose of KB-R7943 had significantly reduced numbers of intact astrocytes detected by GFAP immunoreactivity in the ipsilateral CA2/3 compared to a similar region in the control group (vehicle contralateral). The numbers of intact GFAP-labeled astrocytes in the two higher doses of KB-R7943 were not statistically different from the counts in the control group (vehicle contralateral). *$p < 0.05$ compared to the control group (vehicle contralateral); **$p < 0.01$ compared to the control group (vehicle contralateral).

[F(4,45) = 5.61, $p < 0.01$] between groups. The numbers of GFAP-labeled astrocytes in the ipsilateral hippocampus of vehicle-treated rats was significantly lower than that in the contralateral control hippocampus ($p < 0.01$), and it was also lower in the rats treated with 0.2 nmoles KB-R7943 ($p < 0.05$). However, at the 2.0 nmoles dose of KB-R7943 the reduction only approached statistical significance ($p = 0.059$) and was not significant with 20.0 nmoles ($p = 0.20$). The mean CE for estimates of GFAP-labeled astrocyte counts was 0.047 ± 0.007. There were no significant differences between the ipsilateral vehicle group and the three KB-R9743 dose groups.

In the contralateral hippocampus there were no significant differences [F(3,36) = 2.07, $p = 0.122$] in the numbers of GFAP-labeled astrocytes between the vehicle group (64,742 ± 2,370) and the 0.2 nmoles (70,830 ± 1,416), the 2.0 nmoles (68,645 ± 1,610), and the 20 nmoles (67,116 ± 1,578) KB-R7943 groups.

EIPA treatment: Astrocytes

As shown in Figure 3, stereological quantification of GFAP-labeled astrocytes revealed significant differences [F(4,26) = 12.83, $p < 0.001$] between groups. The numbers of GFAP-labeled astrocytes in the ipsilateral hippocampus of vehicle-treated rats was significantly lower than that in the contralateral control hippocampus ($p < 0.01$), and was comparable to the reduction measured in rats treated with 2.0, 20.0, and 200 nmoles EIPA ($p < 0.01$). The mean CE for estimates of GFAP-labeled astrocyte counts was 0.065 ± 0.016.

In the contralateral hippocampus there were no significant differences [F(3,20] = 0.653, $p = 0.590$) in the numbers of GFAP-labeled astrocytes between the vehicle group (63,928 ± 4,176) and the 2.0 nmoles (72,729 ± 3,516), the 20.0 nmoles (69,994 ± 6,039), and the 200 nmoles (64,326 ± 6,399) EIPA groups.

Amiloride treatment: Astrocytes

As shown in Figure 4, stereological quantification of GFAP-labeled astrocytes revealed significant differences [F(2,21) = 15.30, $p < 0.001$] between groups. In the vehicle-treated rats, there was a significant reduction in the number of GFAP- immunostained astrocytes in the ipsilateral compared to the contralateral hippocampus control ($p < 0.01$). Amiloride treatment resulted in significantly more GFAP-immunostained astrocytes in the ipsilateral hippocampus compared to the ipsilateral hippocampus of vehicle-treated rats after TBI ($p < 0.02$). Differences between control and amiloride-treated groups approached, but did not reach statistical significance ($p < 0.063$). The CE for estimates of GFAP-labeled astrocyte counts was 0.054 ± 0.015.

In the contralateral hippocampus there were no significant differences [F(2,17) = 0.52, $p = 0.61$] in the numbers of GFAP-labeled astrocytes between vehicle (62,242 ± 3,991), amiloride (62,258 ± 3,094), and uninjured sham controls (67,511 ± 1,552).

Amiloride, EIPA, KB-R7943 treatments: Degenerating neurons

Brightly fluorescing Fluoro-Jade staining neuronal cells were observed in the stratum pyramidale of the CA2 and CA3 regions in the ipsilateral (Fig. 5A,B), but not in the contralateral, dorsal hippocampi (data not shown) at 24 h after TBI. Analysis of stereological quantification of Fluoro-Jade-positive cells (Fig. 5C) revealed significant differences between treatment groups (F[3,27] = 6.245, $p = 0.002$). The number of Fluoro-Jade staining cells in the amiloride-treated

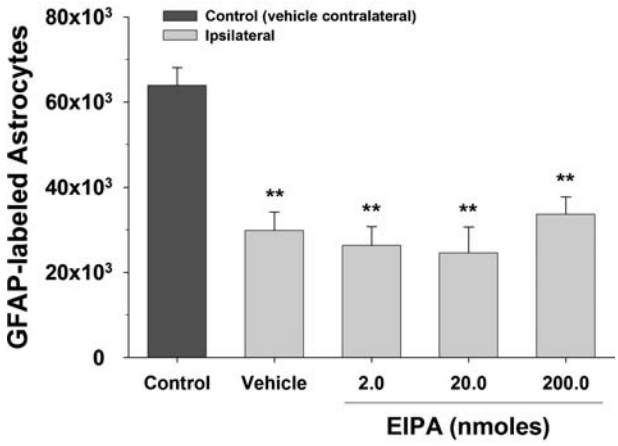

FIG. 3. Stereological quantification of GFAP-labeled astrocytes at 24 h after TBI in hippocampal CA2/3 after EIPA treatment. Vehicle-treated rats and all EIPA dose groups had significantly reduced numbers of intact astrocytes detected by GFAP immunoreactivity in the ipsilateral CA2/3 compared to the analogous region in the control group (vehicle contralateral). EIPA treatment had no effect on GFAP-labeled astrocytes. There were no significant differences in stereological estimates of intact GFAP-labeled astrocytes between any of the EIPA-treated groups and the ipsilateral vehicle group. **$p <$ 0.01 compared to the control group (vehicle contralateral).

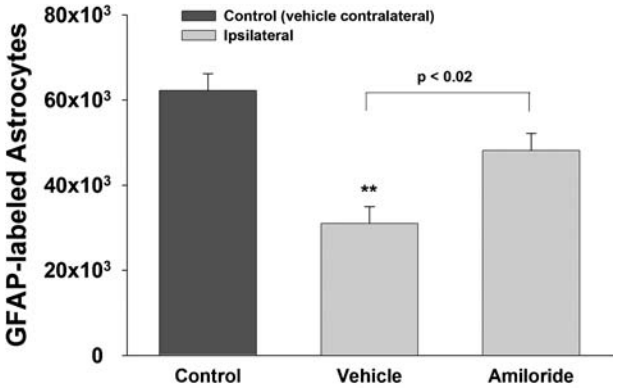

FIG. 4. Stereological quantification of GFAP-labeled astrocytes in hippocampal CA2/3 region after amiloride treatment. Intact astrocytes, as detected by GFAP, were reduced significantly in the CA2/3 region following TBI, as compared with astrocytes in the corresponding region contralateral to the impact in vehicle-treated rats. Amiloride-treatment prior to TBI significantly attenuated the reduced numbers of GFAP-labeled astrocytes. $^{**}p < 0.01$ compared to the control group (vehicle contralateral).

group (708 ± 128) was significantly lower than the vehicle group (1766 ± 236; $p = 0.049$) at 24 h after TBI. The mean CE for estimates of Fluoro-Jade-positive neuron counts was 0.073 ± 0.032.

Discussion

The role of the ion exchangers, NCX and NHE-1, in pathology to astrocytes and neurons following lateral fluid percussion TBI in the rat was examined using several compounds with varying degrees of selectivity. KB-R7943, a preferential inhibitor of the reverse mode of NCX, significantly reduced the loss of GFAP immunoreactivity. EIPA which inhibits NHE-1 (IC_{50} 0.2–0.8 μM) >> ASIC1a (IC_{50} 10–20 μM) (Alexander et al., 2008; Brierley et al., 1994; Wangemann et al., 1996), failed to affect the levels of GFAP immunoreactivity. Amiloride, which inhibits NHE-1 (IC_{50} 10 μM), ASIC1a (IC_{50} 10 μM), and NCX (IC_{50} 690 μM) (Alexander et al., 2008; Kleyman and Cragoe, 1988; Rogister et al., 2001), significantly attenuated the TBI-induced reduction in immunoreactivity to GFAP at 24 h after TBI. Several studies have suggested a link between reduction in GFAP immunoreactivity and astrocyte function and/or survival following TBI (Noble et al., 1992; Zhao et al., 2003) and ischemia (Liu et al., 1999; Ouyang et al., 2007; Petito et al., 1998). The present findings contribute further to our mechanistic understanding of the early changes in the acute compromise of astrocyte structure and function following TBI. Specifically, the KB-R7943 and amiloride results indicate that Ca^{2+} and Na^{+} influx into astrocytes contributes to astrocyte pathology. The lack of EIPA effects suggests that the inward flux of Na^{+} necessary to reverse NCX may utilize other transport mechanisms (e.g., glutamate-sodium co-transport) rather than NHE-1. Indeed, previous results demonstrated that inhibiting glutamate transport with TBOA (DL-threo-beta-benzyloxyaspartate) in mechanically injured astrocyte cultures significantly re-

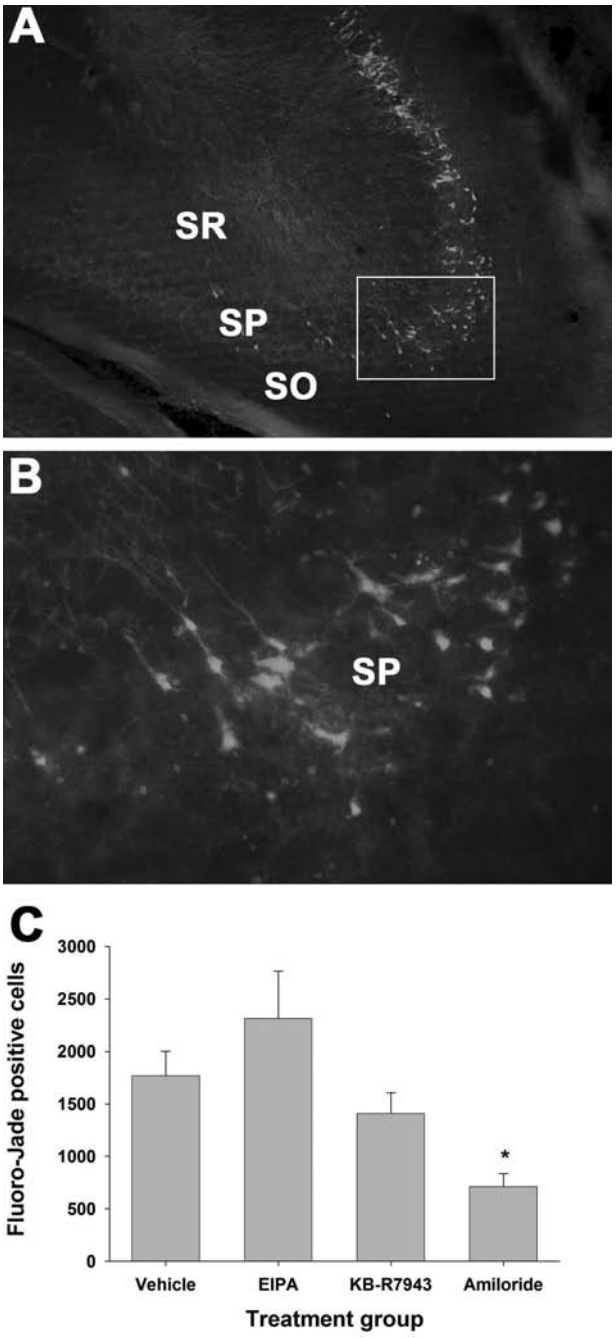

FIG. 5. Fluoro-Jade histofluorescence of degenerating neurons in the hippocampus at 24 h after TBI. (**A**) Representative section from the ipsilateral hemisphere (Bregma −3.80 mm) showing fluorescing cells indicating degenerating neurons in the stratum pyramidale. Scale bar = 100 μm. (**B**) Higher magnification from the boxed area in A shows pyramidal cell bodies and dendrites fluorescing. Scale bar = 10 μm. SO, stratum oriens; SP, stratum pyramidale; SR, stratum radiatum. (**C**) Degenerating neurons were quantified using stereological techniques. Amiloride (100 nmoles) significantly reduced the numbers of Fluoro-Jade-labeled degenerating neurons in the hippocampal CA2/3 region. Compared to vehicle, neither EIPA (200 nmoles) nor KB-R7943 (20 nmoles) significantly affected the numbers of degenerating neurons. $^{*}p < 0.05$ compared to the vehicle contralateral control group. (Color image is available online at www.liebertpub.com/jon)

duced both $[Na^+]_i$ and cell death (Floyd et al., 2005). In contrast to the poly-pharmacological protection of astrocytes, only amiloride significantly reduced neuronal degeneration at 24 h post-injury. This suggests that other inhibitory activities of amiloride, notably ACIC1a (Cho and Askwith, 2008), may contribute to this neuroprotective effect. The inability of more selective NCX or NHE-1 inhibitors (KB-R7943, EIPA) to protect neurons is consistent with the idea that inward movement of sodium from multiple cellular mechanisms contribute to neuronal demise. The data suggest that a combination of reversal of NCX, activation of NHE-1, and possibly activation of ASIC1a significantly contributes to acute neuronal degeneration following TBI.

The present study suggests that astrocytes undergo pathological changes in selectively vulnerable areas such as the hippocampus CA2/3 region following TBI. While quantification of results was restricted to the CA2/3 region of hippocampus in this study, pathological changes to astrocytes in other regions such as the ipsilateral cortex likely occur. Astrocyte vulnerability could be due in part to TBI-induced shifts in ionic concentrations. For example, astrocytic swelling can be a prominent component of cellular ("cytotoxic") brain edema following a shift in water to the intracellular compartment as a result of osmolarity shifts from ion movements (Kimelberg, 1992; Kimelberg et al., 1992). Astrocyte swelling is an acute response to both experimental closed head trauma (Bakay et al., 1977; Nelson et al., 1982) and experimental cerebral ischemia (Jenkins et al., 1984). Cortical biopsies of human head injury complicated with subdural hematoma have shown severe astrocytic edema, dissociation of the perivascular astrocyte endfeet from the capillary basement membrane, and disruption of inter-astrocyte gap junctions (Castejon, 1998). Electron microscopy of brain tissue from human cerebral contusion patients has revealed evidence of astrocytic swelling as early as 3 h after injury, persisting for as long as 3 days (Bullock et al., 1991). While the acute reduction in GFAP immunoreactivity and early astrocyte swelling occur in temporal proximity, the relationship between the two events remains uncertain.

Contribution of the reverse mode of NCX to TBI

Highly elevated $[Na^+]_i$ can have several detrimental consequences including reversal of NCX (Bondarenko and Chesler, 2001; Enkvist et al., 1989). Recent *in vitro* studies demonstrate that moderate to severe mechanical injury or excitotoxic glutamate application (1 mM) to astrocyte cultures produces elevations in $[Na^+]_i$ that are sufficient to cause reversal of NCX (Floyd et al., 2005). In those studies, KB-R7943 applied prior to either glutamate challenge or moderate to severe mechanical strain injury significantly reduced the rise in intracellular calcium in astrocyte cultures and reduced astrocyte death (Floyd et al., 2005). Other studies have shown that inhibition of NCX reversal with KB-R7943 is protective after oxygen and glucose deprivation (MacGregor et al., 2003), after ischemic injury in brain (Pilitsis et al., 2001a), and in hippocampal organotypic brain slices (Breder et al., 2000; Schroder et al., 1999). Thus, the present results are consistent with *in vitro* and *in vivo* studies suggesting that reversal of NCX leads to exacerbation of pathological processes in CNS insults and that inhibition of the NCX can reduce pathology.

Differing results by Amiloride and EIPA

The effects observed with EIPA and amiloride were discrepant; EIPA afforded no protection while amiloride provided protection of both astrocytes (preserved GFAP immunoreactivity) and neurons (reduced Fluoro-Jade histofluorescence). These different effects were likely related to their differential pharmacological actions. EIPA is a more potent derivative of amiloride that inhibits NHE-1 in multiple cell types (Vigne et al., 1983) and also inhibits mitochondrial NHE (Bernardinelli et al., 2006). In contrast, amiloride not only inhibits NHE-1, but also includes varying inhibitory effects on Na^+ channels (Chattou et al., 2000), on NCX (Siegl et al., 1984), and on ASIC1a (Wemmie et al., 2006). EIPA was examined here as a cellular protectant for TBI as it has been reported to impede Na^+ and Ca^{2+} influx and reduce cerebral and myocardial ischemia (Andreeva et al., 1992) and to protect against glutamate-induced cerebellar granule cell death *in vitro* (Andreeva et al., 1992). In a series of studies from Phillis and colleagues, EIPA blocked ischemia-evoked amino acid release from the cortex of ischemic rats (Phillis et al., 1998), reduced ischemia/reperfusion injury to CA1 pyramidal neurons in the gerbil (Phillis et al., 1999), and reduced the efflux of free-fatty acids during reperfusion (Phillis et al., 2000, 2001b). However, the lack of protection afforded by EIPA in the present study suggests that inward Na^+ movement by NHE-1 is not the dominant mechanisms initiating astrocyte or neuronal damage in the hippocampus following moderate fluid percussion TBI. Sodium entry occurs by several mechanisms and our previous *in vitro* studies suggest that glutamate transporters play a prominent role in elevating $[Na^+]_i$ in astrocytes (Floyd et al., 2005). Excessive glutamate release is a hallmark of TBI (Faden et al., 1989; Katayama et al., 1990; Zhong et al., 2006) and each molecule of glutamate taken up during transport is accompanied by three Na^+ ions. The resulting elevated $[Na^+]_i$ activates Na^+/K^+ ATPase with ATP consumption leading to increased glycolysis (Magistretti and Pellerin, 1996; Pellerin and Magistretti, 1994; Silver et al., 1997; Silver and Erecinska, 1997) and subsequent detrimental intracellular acidosis (Kempski et al., 1990; Marmarou, 1992). Neuronal protection by amiloride was a novel and unexpected finding. It suggests that hippocampal neuronal damage occurs by mechanisms different from that of adjacent astrocytes and may include activation of ASIC1a. Given a recent report in cerebral ischmia (Pignataro et al., 2007), we are currently exploring the contribution of ASIC1a to this mechanism using tarantula toxin psalmotoxin, PcTX.

Conclusion

In the present *in vivo* study, it is not possible to determine whether these drugs targeting NCX and NHE-1 affected ion exchangers solely on astrocytes or on both astrocytes and neurons. Thus, the significant reduction in neuronal degeneration detected by reduced Fluoro-Jade staining following amiloride treatment (Fig. 5C) may result from inhibiting ion exchangers located on neurons or astrocytes or both. Inhibi-

tion of ASIC by amiloride may have also contributed to reduced neuronal degeneration since mice lacking the ASIC1a demonstrate considerable neuroprotection from cerebral ischemia (Xiong et al., 2004). Compared to KB-R7943, amiloride affords more robust reduction of astrocyte pathology. This enhanced protection by amiloride may be attributable to its multiple actions; notably combined blockade of NHE-1, NCX, and ASIC1a.

The data from the present study suggests that the alterations in GFAP immunoreactivity following TBI can be attenuated by either inhibition of the reverse mode of NCX (via KB-R7943) or through combined inhibition of NHE-1, NCX, and possibly ASIC1a (via amiloride). The lack of effect by the more selective NHE-1 inhibitor (EIPA) suggests that reversal of NCX may be a key participant resulting in astrocyte pathology. This is consistent with recent *in vitro* evidence demonstrating that KB-R7943 reduced astrocyte death following mechanical injury (Floyd et al., 2005). The protection afforded by pre-injury application of amiloride, a drug with actions at multiple ion exchangers, suggests that alterations in intracellular ionic milieu can have pathological consequences for both astrocytes and neurons following TBI.

Acknowledgments

This research was supported by the National Institutes of Health (grants NS29995 and NS45136 to B.G.L.; NS39090 to R.F.B.; NS40489 to F.A.G.) and the University of California CRCC (grant to F.A.G.).

Author Disclosure Statement

No conflicting financial interests exist.

References

Alexander, S.P., Mathie, A., and Peters, J.A. (2008). Guide to Receptors and Channels (GRAC), 3rd edition. Br. J. Pharmacol. 153, Suppl 2, S1–S209.

Andreeva, N., Khodorov, B., Stelmashook, E., Sokolova, S., Cragoe, E., Jr., and Victorov, I. (1992). 5–(N-ethyl-N-isopropyl)amiloride and mild acidosis protect cultured cerebellar granule cells against glutamate-induced delayed neuronal death. Neuroscience 49, 175–181.

Bakay, L., Lee, J.C., Lee, G.C., and Peng, J.R. (1977). Experimental cerebral concussion. Part 1: An electron microscopic study. J. Neurosurg. 47, 525–531.

Bernardinelli, Y., Azarias, G., and Chatton, J.Y. (2006). In situ fluorescence imaging of glutamate-evoked mitochondrial Na^+ responses in astrocytes. Glia 54, 460–470.

Bondarenko, A., and Chesler, M. (2001). Calcium dependence of rapid astrocyte death induced by transient hypoxia, acidosis, and extracellular ion shifts. Glia 34, 143–149.

Breder, J., Sabelhaus, C.F., Opitz, T., Reymann, K.G., and Schroder, U.H. (2000). Inhibition of different pathways influencing Na^+ homeostasis protects organotypic hippocampal slice cultures from hypoxic/hypoglycemic injury. Neuropharmacology 39, 1779–1787.

Brierley, G.P., Baysal, K., Jung, and D.W. (1994). Cation transport systems in mitochondria: Na^+ and K^+ uniporters and exchangers. J. Bioenerg. Biomembr. 26, 519–526.

Bullock, R., Maxwell, W.L., Graham, D.I., Teasdale, G.M., and Adams, J.H. (1991). Glial swelling following human cerebral contusion: an ultrastructural study. J. Neurol. Neurosurg. Psychiatry 54, 427–434.

Castejon, O.J. (1998). Morphological astrocytic changes in complicated human brain trauma. A light and electron microscopic study. Brain Inj. 12, 409–427.

Chattou, S., Coulombe, A., Diacono, J., Le Grand, B., John, G., and Feuvray, D. (2000). Slowly inactivating component of sodium current in ventricular myocytes is decreased by diabetes and partially inhibited by known Na^+-H^+ exchange blockers. J. Mol. Cell Cardiol. 32, 1181–1192.

Cho, J.H., and Askwith, C.C. (2008). Presynaptic release probability is increased in hippocampal neurons from ASIC1 knockout mice. J. Neurophysiol. 99, 426–441.

Danbolt, N.C. (1994). The high affinity uptake system for excitatory amino acids in the brain. Prog. Neurobiol. 44, 377–396.

Danbolt, N.C. (2001). Glutamate uptake. Prog. Neurobiol. 65, 1–105.

Dixon, C.E., Lyeth, B.G., Povlishock, J.T., Findling, R.L., Hamm, R.J., Marmarou, A., Young, H.F., and Hayes, R.L. (1987). A fluid percussion model of experimental brain injury in the rat. J. Neurosurg. 67, 110–119.

Enkvist, M.O., Holopainen, I., and Akerman, K.E. (1989). Glutamate receptor-linked changes in membrane potential and intracellular Ca^{2+} in primary rat astrocytes. Glia 2, 397–402.

Faden, A.I., Demediuk, P., Panter, S.S., and Vink, R. (1989). The role of excitatory amino acids and NMDA receptors in traumatic brain injury. Science 244, 798–800.

Floyd, C.L., Gorin, F.A., and Lyeth, B.G. (2005). Mechanical strain injury increases intracellular sodium and reverses Na^+/Ca^+ exchange in cortical astrocytes. Glia 51, 35–46.

Floyd, C.L., and Lyeth, B.G. (2007). Astroglia: important mediators of traumatic brain injury, in: J.T. Weber, A.I. R. Maas, Eds., *Neurotrauma: New Insights into Pathology and Treatment. Progress in Brain Research, Vol. 161*. Elsevier: Amsterdam, pps. 61–79.

Globus, M.Y.T., Alonso, O., Dietrich, W.D., Busto, R., and Ginsberg, M.D. (1995). Glutamate release and free radical production following brain injury: effects of posttraumatic hypothermia. J. Neurochem. 65, 1704–1711.

Grinstein, S., and Rothstein, A. (1986). Mechanisms of regulation of the Na^+/H^+ exchanger. J. Membr. Biol. 90, 1–12.

Gundersen, H.J. (1986). Stereology of arbitrary particles. A review of unbiased number and size estimators and the presentation of some new ones, in memory of William R. Thompson. J. Microsc. 143, 3–45.

Hallam, T.M., Floyd, C.L., Folkerts, M.M., Lee, L.L., Gong, Q.Z., Lyeth, B.G., Muizelaar, J.P., and Berman, R.F. (2004). Comparison of behavioral deficits and acute neuronal degeneration in rat lateral fluid percussion and weight-drop brain injury models. J. Neurotrauma 21, 521–539.

Jenkins, L.W., Becker, D.P., and Coburn, T.H. (1984). A quantitative analysis of glial swelling and ischemic neuronal injury following cerebral ischemia, in: T.G. Go, A. Baethmann, Eds., *Recent Progress in the Study and Therapy of Brain Edema*. Plenum Press: New York, pps. 523–537.

Katayama, Y., Becker, D.P., Tamura, T., and Hovda, D.A. (1990). Massive increases in extracellular potassium and the indiscriminate release of glutamate following concussive brain injury. J. Neurosurg. 73, 889–900.

Kempski, O., Staub, F., Jansen, M., and Baethmann, A. (1990). Molecular mechanisms of glial cell swelling in acidosis. Adv. Neurol. 52, 39–45.

Kimelberg, H.K. (1992). Astrocytic edema in CNS trauma. J. Neurotrauma 9, S71–S81.

Kimelberg, H.K., Jalonen, T., and Walz, W. (1992). Regulation of the brain microenvironment: transmitter and ions, in: S. Murphy, Ed., *Astrocytes: Pharmacology and Function*. Academic Press: Orlando, FL.

Kleyman, T.R., and Cragoe, E.J., Jr. (1988). Amiloride and its analogs as tools in the study of ion transport. J. Membr. Biol. 105, 1–21.

Liu, D., Smith, C.L., Barone, F.C., Ellison, J.A., Lysko, P.G., Li, K., and Simpson, I.A. (1999). Astrocytic demise precedes delayed neuronal death in focal ischemic rat brain. Brain Res. Mol. Brain Res. 68, 29–41.

MacGregor, D.G., Avshalumov, M.V., and Rice, M.E. (2003). Brain edema induced by in vitro ischemia: causal factors and neuroprotection. J. Neurochem. 85, 1402–1411.

Magistretti, P.J., and Pellerin, L. (1996). Cellular bases of brain energy metabolism and their relevance to functional brain imaging: evidence for a prominent role of astrocytes. Cereb. Cortex 6, 50–61.

Marmarou, A. (1992). Intracellular acidosis in human and experimental brain injury. J. Neurotrauma. 9, Suppl 2, S551–s562.

McIntosh, T.K., Faden, A.I., Bendall, M.R., and Vink, R. (1987). Traumatic brain injury in the rat: alterations in brain lactate and pH as characterized by ^{1}H and ^{31}P nuclear magnetic resonance. J. Neurochem. 49, 1530–1540.

McIntosh, T.K., Vink, R., Noble, L., Yamakami, I., Fernyak, S., Soares, H., and Faden, A.I. (1989). Traumatic brain injury in the rat: characterization of a lateral fluid-percussion model. Neuroscience 28, 233–244.

Myer, D.J., Gurkoff, G.G., Lee, S.M., Hovda, D.A., and Sofroniew, M.V. (2006). Essential protective roles of reactive astrocytes in traumatic brain injury. Brain 129, 2761–2772.

Nelson, L.R., Auen, E.L., and Bourke, R.S. (1982). A comparison of animal head injury models developed for treatment modality evaluation, in: R. Grossman, G.P.L., Eds., *Head Injury: Basic and Clinical Aspects*. Raven Press: New York, pps. 117–127.

Noble, L.J., Hall, J.J., Chen, S., and Chan, P.H. (1992). Morphologic changes in cultured astrocytes after exposure to glutamate. J. Neurotrauma 9, 255–267.

Ouyang, Y.B., Voloboueva, L.A., Xu, L.J., and Giffard, R.G. (2007). Selective dysfunction of hippocampal CA1 astrocytes contributes to delayed neuronal damage after transient forebrain ischemia. J. Neurosci. 27, 4253–4260.

Pellerin, L., and Magistretti, P.J. (1994). Glutamate uptake into astrocytes stimulates aerobic glycolysis: a mechanism coupling neuronal activity to glucose utilization. Proc. Natl. Acad. Sci. USA 91, 10625–10629.

Petito, C.K., Olarte, J.P., Roberts, B., Nowak, T.S., Jr., and Pulsinelli, W.A. (1998). Selective glial vulnerability following transient global ischemia in rat brain. J. Neuropathol. Exp. Neurol. 57, 231–238.

Phillis, J.W., Estevez, A.Y., Guyot, L.L., and O'Regan, M.H. (1999). 5–(N-Ethyl-N-isopropyl)-amiloride, an Na^{+}-H^{+} exchange inhibitor, protects gerbil hippocampal neurons from ischemic injury. Brain Res. 839, 199–202.

Phillis, J.W., O'Regan, M.H., and Song, D. (1998). 5-(N-Ethyl-N-isopropyl)-amiloride inhibits amino acid release from the ischemic rat cerebral cortex: role of Na^{+}-H^{+} exchange. Brain Res. 812, 297–300.

Phillis, J.W., Ren, J., and O'Regan, M.H. (2000). Inhibition of Na^{+}/H^{+} exchange by 5-(N-ethyl-N-isopropyl)-amiloride reduces free fatty acid efflux from the ischemic reperfused rat cerebral cortex. Brain Res. 884, 155–162.

Pignataro, G., Simon, R.P., and Xiong, Z.G. (2007). Prolonged activation of ASIC1a and the time window for neuroprotection in cerebral ischaemia. Brain 130, 151–158.

Pilitsis, J.G., Diaz, F.G., O'Regan, M.H., and Phillis, J.W. (2001a). Inhibition of Na^{+}/Ca^{+} exchange by KB-R7943, a novel selective antagonist, attenuates phosphoethanolamine and free fatty acid efflux in rat cerebral cortex during ischemia-reperfusion injury. Brain Res. 916, 192–198.

Pilitsis, J.G., Diaz, F.G., O'Regan, M.H., and Phillis, J.W. (2001b). Inhibition of Na^{+}/H^{+} exchange by SM-20220 attenuates free fatty acid efflux in rat cerebral cortex during ischemia-reperfusion injury. Brain Res. 913, 156–158.

Rogister, F., Laeckmann, D., Plasman, P., Van Eylen, F., Ghyoot, M., Maggetto, C., Liegeois, J., Geczy, J., Herchuelz, A., Delarge, J., and Masereel, B. (2001). Novel inhibitors of the sodium-calcium exchanger: benzene ring analogues of N-guanidino substituted amiloride derivatives. Eur. J. Med. Chem. 36, 597–614.

Schmued, L.C., Albertson, C., and Slikker, W.J. (1997). Fluoro-Jade: a novel fluorochrome for the sensitive and reliable histochemical localization of neuronal degeneration. Brain Res. 751, 37–46.

Schmued, L.C., and Hopkins, K.J. (2000). Fluoro-Jade: novel fluorochromes for detecting toxicant-induced neuronal degeneration. Toxicol. Pathol. 28, 91–99.

Schroder, U.H., Breder, J., Sabelhaus, C.F., and Reymann, K.G. (1999). The novel Na^{+}/Ca^{2+} exchange inhibitor KB-R7943 protects CA1 neurons in rat hippocampal slices against hypoxic/hypoglycemic injury. Neuropharmacology 38, 319–321.

Siegl, P.K., Cragoe, E.J., Jr., Trumble, M.J., and Kaczorowski, G.J. (1984). Inhibition of Na^{+}/Ca^{2+} exchange in membrane vesicle and papillary muscle preparations from guinea pig heart by analogs of amiloride. Proc. Natl. Acad. Sci. USA 81, 3238–3242.

Silver, I.A., Deas, J., and Erecinska, M. (1997). Ion homeostasis in brain cells: differences in intracellular ion responses to energy limitation between cultured neurons and glial cells. Neuroscience 78, 589–601.

Silver, I.A., and Erecinska, M. (1997). Energetic demands of the Na^{+}/K^{+} ATPase in mammalian astrocytes. Glia 21, 35–45.

Sterio, D.C. (1984). The unbiased estimation of number and sizes of arbitrary particles using the disector. J. Microsc. 134, 127–136.

Takahashi, M., Billups, B., Rossi, D., Sarantis, M., Hamann, M., and Attwell, D. (1997). The role of glutamate transporters in glutamate homeostasis in the brain. J. Exp. Biol. 200, 401–409.

Vigne, P., Frelin, C., Cragoe, E.J., Jr., and Lazdunski, M. (1983). Ethylisopropyl-amiloride: a new and highly potent derivative of amiloride for the inhibition of the Na^{+}/H^{+} exchange system in various cell types. Biochem. Biophys. Res. Commun. 116, 86–90.

Vink, R., McIntosh, T.K., Weiner, M.W., and Faden, A.I. (1987). Effects of traumatic brain injury on cerebral high-energy phosphates and pH: a ^{31}P magnetic resonance spectroscopy study. J. Cereb. Blood Flow Metab. 7, 563–571.

Wangemann, P., Liu, J., and Shiga, N. (1996). Vestibular dark cells contain the Na^{+}/H^{+} exchanger NHE-1 in the basolateral membrane. Hearing Res. 94, 94–106.

Wemmie, J.A., Price, M.P., and Welsh, M.J. (2006). Acid-sensing ion channels: advances, questions and therapeutic opportunities. Trends Neurosci. 29, 578–586.

West, M.J., Slomianka, L., and Gundersen, H.J. (1991). Unbiased

stereological estimation of the total number of neurons in the-subdivisions of the rat hippocampus using the optical fractionator. Anat. Rec. 231, 482–497.

Xiong, Z.G., Zhu, X.M., Chu, X.P., Minami, M., Hey, J., Wei, W.L., MacDonald, J.F., Wemmie, J.A., Price, M.P., Welsh, M.J., and Simon, R.P. (2004). Neuroprotection in ischemia: blocking calcium-permeable acid-sensing ion channels. Cell 118, 687–698.

Zhao, X., Ahram, A., Berman, R.F., Muizelaar, J.P., and Lyeth, B.G. (2003). Early loss of astrocytes after experimental traumatic brain injury. Glia 44, 140–152.

Zhong, C., Zhao, X., Van, K.C., Bzdega, T., Smyth, A., Zhou, J., Kozikowski, A.P., Jiang, J., O'Connor, W.T., Berman, R.F., Neale, J.H., and Lyeth, B.G. (2006). NAAG peptidase inhibitor increases dialysate NAAG and reduces glutamate, aspartate and GABA levels in the dorsal hippocampus following fluid percussion injury in the rat. J. Neurochem. 97, 1015–1025.

Address reprint requests to:
Bruce G. Lyeth, Ph.D.
Department of Neurological Surgery
University of California at Davis
1515 Newton Court
One Shields Avenue
Davis, CA 95616-8797

E-mail: bglyeth@ucdavis.edu